VERSITA

Photo fenton like process Fe^{3+}/$(NH_4)_2S_2O_8$/UV for the degradation of Di azo dye congo red using low iron concentration

Research Article

L. Gomathi Devi*, S. Girish Kumar, K. Mohan Reddy

*Department of Post Graduate Studies in Chemistry,
Central College City Campus, Bangalore University,
Bangalore-560 001, India.*

Abstract: Degradation of Congo Red (CR) a di azo dye in aqueous solution is investigated by a Photo Fenton like process using Fe^{3+} ions as the catalyst and peroxy disulfate as the oxidant. The influence of various reaction parameters like, concentration of Fe^{3+} ions, concentration of the dye, concentration of ammonium persulfate, pH of the solution and the presence of hydroxyl radical scavenger are studied and optimal conditions are reported. The degradation rate decreased at higher dye concentration and at higher pH. The rate constant (k), catalytic efficiency (k_c) and process efficiency (Φ) are evaluated for different concentration of Fe^{3+} ions. The degradation of CR by the photo Fenton like process leads to the formation of 4-Amino, 3-azo naphthalene sulphonic acid, dihydroxy substituted naphthalene, dihydroxy substituted biphenyl, phenol, quinol etc., as intermediates, based on which probable degradation mechanism is proposed. These results show that a photo Fenton like process could be useful technology for the mineralization of di azo dyes under lower concentration of iron in acidic conditions. The present process is advantageous as it lowers the sludge production resulting from the iron complex.

Keywords: *Fenton like process • Ammonium persulfate • Congo Red • Spectroscopic analysis • Photodegradation*

1. Introduction

The textile industry produces large quantities of dye effluents that contain significant concentrations of organic dyes. These effluents directly enter into the rivers and other water resources. The difficulty in treating these dye effluents arises from several factors, which are characteristic of most textile industry waste streams. The effluents contain dyes that come from different production lines, and can therefore vary significantly in their qualities. The removal of these dyes from the wastewater is a great challenge for the related industries, since they are persistent in nature and difficult to destroy by ordinary treatment methods, especially in ppm and ppb concentrations. Among the various dyes used, azo dyes constitute about 80% of the reactive dyes. The traditional methods of removing these dyes by various processes like carbon adsorption, activated sludge treatment, membrane filtration, flocculation and reverse osmosis are inefficient, and

has further disadvantage of secondary pollutions. These processes transfer pollutants from one phase to another phase. Ozone and hypochlorite oxidation are efficient decolorizing methods, but they are very expensive and tedious processes. Further secondary pollution arising from residual chlorine adds to the problem [1]. In recent years, Advanced Oxidation Processes (AOPs) is the field of interest for the degradation of these dyes. The reason for the popularity of AOPs is mainly due to the inability of biological processes to treat highly contaminated and toxic waste water. There are three categories of AOPs: (1) UV/O_3; (2) Photo catalysis (TiO_2 or other semiconductor particles under UV illumination); (3) Fenton process (Fe^{2+} / H_2O_2), Photo Fenton process (Fe^{2+} / H_2O_2 / UV) and Photo Fenton like processes of homogeneous nature (Fe^{3+}/ H_2O_2 / UV, Fe^{3+}/ APS / UV and Fe^{2+}/ APS / UV) and heterogeneous nature (Fe^0 / oxidants) (where APS is $(NH_4)_2S_2O_8$). The present Research mainly focuses on the mineralization of Congo Red (CR) a di azo dye by

* E-mail: gomatidevi_naik@yahoo.co.in

homogeneous Photo Fenton like process. The presence of two azo groups makes the dye molecule more inert. Photo catalytic degradation of azo dyes seems to be significantly influenced by their polar nature, the number of azo bonds present in the dye molecule and the types of auxiliary groups attached to the azo bond. The triazo dyes are most difficult to degrade and the monoazo are easy to degrade, while the degradation of di azo dyes lies in between. The partial degradation of di azo dyes produces a mixture of substituted mono azo benzene, partially reduced di azo benzene and many more intermediates. CR has a strong affinity for protein material and cellulose. Its industrial uses include the dyeing of leather and paper. CR is a simple benzidine di azo dye. This red dye changes to blue when converted to disodium salt (process of salting out with NaCl). The red salt is used extensively to dye cotton directly.

The Photo Fenton process involves the production of hydroxyl radicals *in situ*, which is characterized by the non-selectivity in their attack. Hydroxyl radicals have a very high oxidizing power (2.8 V) next only to fluorine and mineralize most of the organic dyes to CO_2 and H_2O. Fenton's process has proved to be promising, efficient, cost effective and an attractive treatment method for the effective degradation of dyes and hazardous organic pollutants [2-17]. The advantages of this process are that it is simple, and easy to operate; the reactions can be carried out under laboratory conditions. The advantages of this process over other oxidation process are that reagents are easily available, cheap and cost effective. Further no scattering of light takes place, contact between pollutants and the catalyst is high since reaction is homogeneous. The main disadvantage of this process is that the reaction proceeds efficiently only under acidic conditions; since under alkaline pH, iron precipitates as iron hydroxide. Secondly, removal of sludge containing iron ions at the end of the process is costly and needs a large amount of chemicals and man power. In view of this, the present research overcomes such disadvantages by using very low concentration of Fe^{3+} ions. Azo dyes are not biodegradable by aerobic treatment process [18]. However, under anaerobic conditions azo dyes can be decolorized [19-20] by reducing the azo bond to the potentially carcinogenic aromatic amines [21]. Therefore, its mineralization by this simple and cost effective photo Fenton like process is important.

2. Experimental Procedures

2.1 Materials

Ferric Chloride ($FeCl_3$) and methanol were supplied by Merck. Concentrated nitric acid and ammonium persulphate (APS) were obtained from SD Fine Chemicals, Bombay. The di azo dye Congo Red (CR) was obtained from Aldrich. The molecular formula of Congo Red is $C_{32}H_{22}N_6O_6S_2Na_2$ and formula weight is 697. The other names of Congo Red are direct red and cotton red. The structure of the Congo Red is shown in Fig. 1.

2.2 Irradiation procedure

Photo Fenton reactions were carried out at room temperature using a thermostat in a circular pyrex glass reactor with a diameter of 150 mm, a height of 75 mm, and a surface area found to be 176.6 cm². Artificial light source used in the present study is 125 W medium pressure mercury vapor lamp. The photon flux of the light source is 7.75 mW cm⁻², as determined by ferri oxalate actinometry for the wavelengths around 350 - 400 nm. The lamp was warmed for 10 minutes to reach a constant output. The emitting light was focused directly without any filters at a distance of 29 cm. All the experiments were performed using distilled water. The pH of solution was adjusted by adding either dilute NaOH or dilute H_2SO_4 and measured using a Systronics Digital pH meter.

2.3 Analysis

The extent of degradation was followed by Schimadzu UV-1700 pharmaspec UV-visible double beam spectrophotometer. The reference used in the UV-vis spectral analysis had all the ingredients including Fe^{3+} solution except CR. The resultant spectrum obtained is the subtraction effect to eliminate the influence of Fe^{3+} ions on the CR molecule. The centrifugates were extracted into non-aqueous medium and 1 µL was
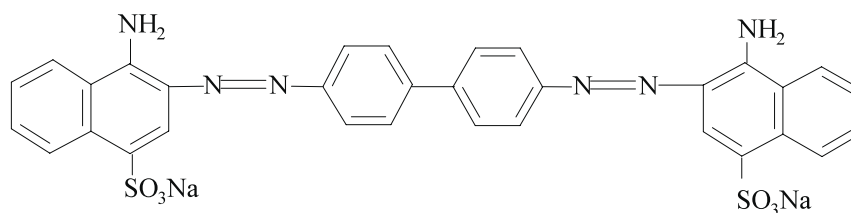

Figure 1. Structure of Congo Red (CR) dye.

Photo fenton like process Fe³⁺/(NH₄)₂S₂O₈/UV
for the degradation of Di azo dye congo red
using low iron concentration

injected to GC-MS analysis (using GC-MS-QP-5000 Schimadzu) and Thermo Electron Trace GC ultra coupled to a DSQ mass spectrometer equipped with an Alltech ECONO-CAP-EC-5 capillary column (30 m × 0.25 mm *i.d.* × 0.25 mm film thickness) was used. Pure helium was used as the carrier gas at a flow rate of 1.2 mL min⁻¹. The injector / transfer line / trap temperature was 220 / 250 / 200°C, respectively. Electron impact ionization was carried out at 70 eV and electron current of 60 µA.

3. Results And Discussion

Fenton's process involves the generation of hydroxyl radicals by using Fe^{2+} with oxidizing agent like H_2O_2 or APS. The present research uses Fe^{3+} ions as the catalyst and APS as oxidizing agent. Persulfate can be induced to form sulfate radicals, which provides free radical mechanism similar to the hydroxyl radical pathways generated by Fenton's chemistry. The sulfate radical is a strong oxidizing species in aqueous media with a redox potential of 2.6 V. It is next to the hydroxyl free radical whose redox potential is 2.8 V. In addition to its oxidizing strength, persulfate and sulfate radicals have several advantages over other oxidant systems. First, it is kinetically fast. Second, it is more stable than the hydroxyl radical and thus able to transport greater distances. Third, persulfate provides better acidic pH necessary for Fenton's process. These attributes combine to make the persulfate a viable option for the chemical oxidation of a broad range of contaminants. A number of ways to generate hydroxyl radicals under acidic pH in Fe^{3+} / APS system can be summarized as follows

Fe^{3+} reacts with persulfate anions, producing sulfate radicals, and is reduced to Fe^{2+}

$$Fe^{3+} + S_2O_8^{2-} \rightarrow 2SO_4^{-\bullet} + Fe^{2+} \tag{1}$$

Then, the sulfate radicals react with water forming hydroxyl radicals

$$SO_4^{-\bullet} + H_2O \rightarrow SO_4^{2-} + {}^{\bullet}OH + H^+ \tag{2}$$
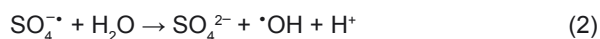
Fe^{3+} ions form an intermediate $[Fe(OH)]^{2+}$, which under UV light generates hydroxyl radicals [3].

$$Fe^{3+} + H_2O \rightarrow [Fe(OH)]^{2+} \tag{3}$$

$$[Fe(OH)]^{2+} \rightarrow Fe^{2+} + {}^{\bullet}OH \tag{4}$$

The photo generated Fe^{2+} reacts with persulfate anions generating sulfate radicals as shown in Eq. 5, which acts as a source for the production of hydroxyl radicals as shown in Eq. 2.

$$Fe^{2+} + S_2O_8^{2-} \rightarrow Fe^{3+} + SO_4^{2-} + SO_4^{-\bullet} \tag{5}$$
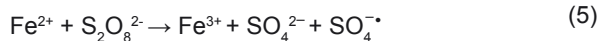
This cyclic process leads to the generation of a greater number of hydroxyl radicals when Fe^{3+} and APS are used under suitable experimental conditions.

3.1 Effect of oxidizing agent

The influence of the oxidizing agent is monitored by keeping Fe^{3+} concentration constant and maintaining the solution pH at 3. Fig. 2 shows the plot of concentration *versus* time for the photo Fenton process at different oxidant concentrations. When the concentration of APS is increased from 20 ppm to 50 ppm, the degradation rate also increased. The visual discoloration of the dye was observed at 50 minutes for 50 ppm APS. The rate of the reaction at 30 minutes is found to be 0.6×10^{-2} ppm min⁻¹ for 20 ppm APS, which increases to 1.8×10^{-2} ppm min⁻¹ for 50 ppm APS. Beyond this optimum concentration degradation rate remains almost constant. The excess radicals generated may undergo recombination or may get involved in the side reactions, which is implied by the overlap of the curves in the Fig. 2 for both 50 and 60 ppm APS . Though more hydroxyl radicals are generated when APS is used as an oxidant, a greater number of protons are also produced simultaneously, as shown in the Eq. 2. The excess protons present in the solution acts as a hydroxyl radical scavenger, as shown in Eq. 6 [22]. Therefore, the APS concentration was optimized to 50 ppm.

$$H^+ + OH^{\bullet} + e^- \rightarrow H_2O \tag{6}$$

3.2 Effect of Fe³⁺

The effect of Fe^{3+} ions was investigated by keeping the oxidant concentration constant (50 ppm APS) and maintaining the solution at pH 3. The rate of the reaction increased when the concentration of Fe^{3+} ions is increased from 2 ppm to 6 ppm. The discoloration of the dye takes 80 minutes for 2 ppm and 50 minutes for 6 ppm of Fe^{3+} ions. Beyond this optimum concentration, the rate of the reaction gradually decreased, as shown in Fig. 3. This is due to an inhibition effect shown by the excess Fe^{2+} ions. The excess Fe^{2+} ions produced during the photo reduction of Fe^{3+} ions (Eqs. 1 and 4) competes for hydroxyl radicals along with dye molecule, as shown in Eq. 7 [22].
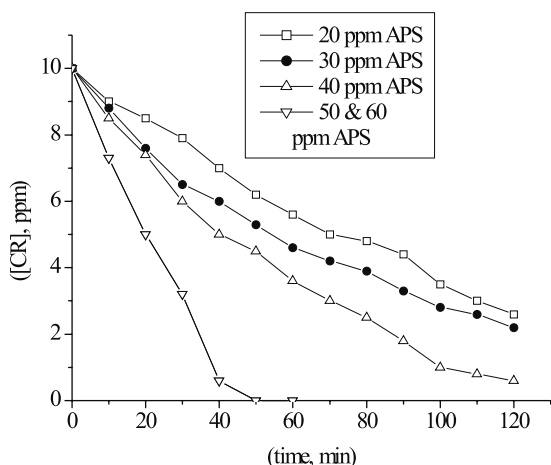
Figure 2. Effect of concentration of oxidizing agent on the degradation of the dye.
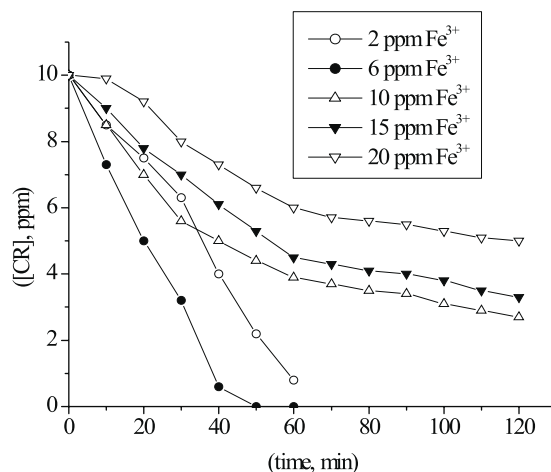

Figure 3. Effect of concentration of Fe^{3+} on the degradation of the dye.

$$Fe^{2+} + OH^• \rightarrow Fe^{3+} + OH^- \qquad (7)$$

This reduces the availability of hydroxyl radical for the dye degradation. Moreover, it is better to optimize the reaction condition with a lower concentration of Fe^{3+} ions so as to avoid sludge production resulting from the formation of the iron complex. The results show a rate of 2.6×10^{-2} ppm min^{-1} when the Fe^{3+} concentration is around 2 - 6 ppm and decreases to 0.9×10^{-2} ppm min^{-1} for higher concentrations of iron.

3.3 Effect of pH

The influence of pH on the decolorization was investigated by keeping the Fe^{3+} concentration and oxidant concentration constant. pH of the solution is an important parameter for the oxidation of pollutants in Fenton's reactions. Kang *et al*. reported that the photo Fenton process is more effective under acidic conditions, and higher pH values are reported to be unsatisfactory for the oxidation of organic pollutants [16]. Under strong acidic conditions with pH 1.0, the decolorization of the dye is 69%, while at pH 3 it is 100% for 50 minutes of irradiation [1-22], as shown in the Fig. 4. This can be accounted to the fact that, at this pH 3, approximately half of ferrous ions are present in the form of Fe^{3+} ion and half as complex ions of $[Fe(OH)]^{2+}$, which are photo

**Table 1.** Various hydrated iron(III) species in solution as a function of pH.

Fe^{3+} species	pH range
Fe $[H_2O]_6$ $^{3+}$	1-2
Fe $[OH]$ $[H_2O]_5$ $^{2+}$	2-3
Fe $[OH]_2[H_2O]_4$ $^+$	3-4
Fe $[OH]_3$	7-10

active species. Either above or below this pH value, the reaction leads to the decrease in the concentration of $[Fe(OH)]^{2+}$ or it can lead to the precipitation of ferrous ion as oxy hydroxide. Neamtu *et al*. have shown the various photoactive species of iron at different pH values (Table 1). The decrease in the decolorization efficiency at lower pH values, is due to the fact that the excess H^+ ions in the solution may act as hydroxyl radical scavenger as shown in Eq. 6. Beyond the optimum pH 3, the degradation rate decreased, and in alkaline medium the dye almost resisted degradation. This is due to the precipitation of hydroxides of iron at higher pH, which further reduces the generation of hydroxyl radicals.

3.4 Effect of hydroxyl radical scavenger

The generation of hydroxyl radicals and its role in the photo Fenton's degradation mechanism is confirmed by performing the reaction in presence of hydroxyl radical scavenger like methyl alcohol [23]. Methanol reacts with hydroxyl radicals with second order rate constant around 9.7×10^8 mol^{-1} sec^{-1} (Eq. 8).

$$CH_3OH + {}^•OH \rightarrow CH_3O^• + H_2O \qquad (8)$$
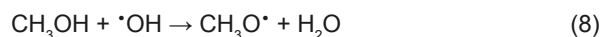
The effect of radical scavenger is shown in Fig. 5. The discoloration of the dye completes in 50 minutes in the absence of alcohol. With increase in the volume of methyl alcohol from 0.5 mL to 3 mL, the decolorization efficiency decreases to 21%, and remains constant even after the addition of 6 mL of alcohol. This is due to the fact that the methyl alcohol can effectively scavenge hydroxyl radicals but not sulfate radicals. The sulfate radical anions produced in the case of APS shows various possible reaction mechanisms in the process of
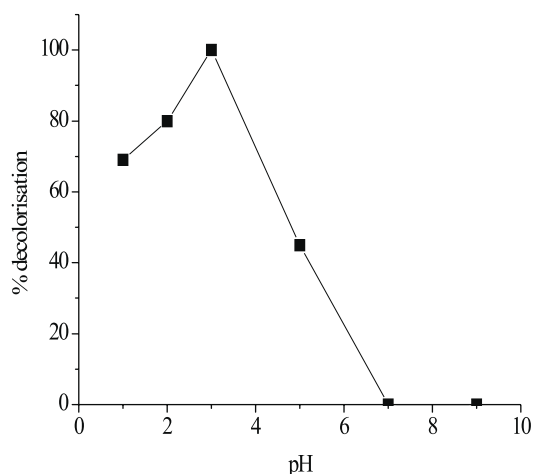
Photo fenton like process $Fe^{3+}/(NH_4)_2S_2O_8/UV$
for the degradation of Di azo dye congo red
using low iron concentration

Figure 4. Influence of pH on the decolorisation rate.
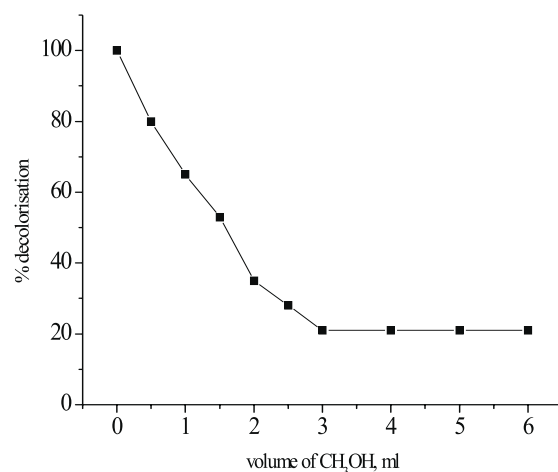

Figure 5. Plot of % decolorisation *versus* volume of methyl alcohol.
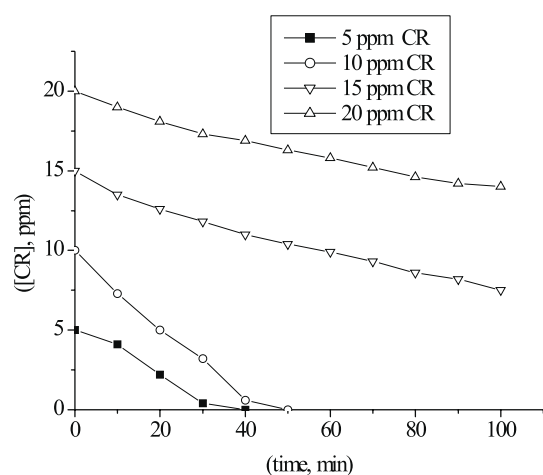

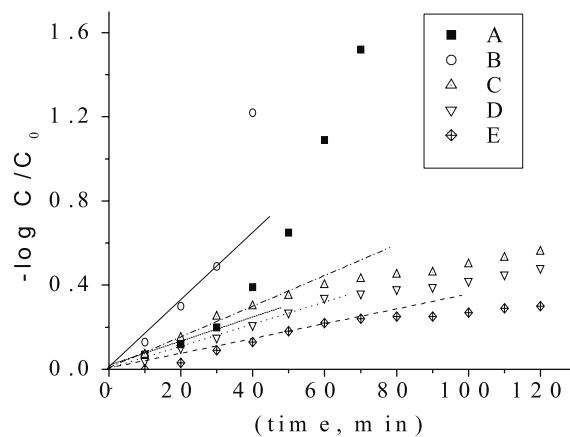**Figure 6.** Effect of initial concentration of the dye.

Figure 7. Plot of -log C/C_0 *versus* time for the degradation of CR at various concentration of Fe^{3+} catalyst. A) 2 ppm Fe^{3+}, B) 6 ppm Fe^{3+}, C) 10 ppm Fe^{3+}, D) 15 ppm Fe^{3+} and E) 20 ppm Fe^{3+}.

degradation: (i) Abstraction of hydrogen atom from the saturated carbon; (ii) Sulfate radical is capable of adding itself to the unsaturated compounds; (iii) Sulfate radical can also remove an electron from the anions and neutral molecules [24]. Hence the observed decolorization (21%) was due to the presence of sulfate radicals [25]. The rate of the reaction decreases from 2.6×10^{-2} to 0.2×10^{-2} ppm min^{-1} in the presence of alcohol (3 mL). This provides an evidence for the role of hydroxyl radical in the photo degradation process.

3.5 Effect of initial concentration of the dye

Initial concentration of the dye plays a major role and has a significant influence on the degradation rate. Fig. 6 shows the effect of initial concentration of the dye. The complete discoloration of the dye was achieved in

30 minutes for 5 ppm, and 50 minutes for 10 ppm dye concentration. When the concentration of the dye is further increased to 15 and 20 ppm, only 66% and 20% of the dye gets decolorized in one hour of UV irradiation. This observed decrease in the rate can be explained in the following way: (i) as the dye concentration is increased, the rate of generation of hydroxyl radicals will not increase proportionally; (ii) high dye concentration can reduce the UV light penetration into the depth of the solution which decreases the rate of generation of hydroxyl radicals; (iii) due to insufficient availability of oxidizing agent the degradation rate may further decrease [26-27]; (iv) at high dye concentration Fe^{3+} ions gets shielded from absorbing UV light resulting in the abrupt termination of photo oxidation reaction; (v) there may be other reactions initiated at high

concentration of the dye like dimerization, complex formation *etc*., which further complicates the reaction mechanism. The rate of the degradation for 5 ppm CR is 3.6×10^{-2} ppm min^{-1}, while for 10 ppm it is 1.8×10^{-2} ppm min^{-1}. With further increase in dye concentration to 20 ppm the rate drastically decreases to 0.4×10^{-2} ppm min^{-1}. These results show that the photo Fenton process is more effective in treating the water containing lower concentration of the dye.

3.6 Kinetic Studies

Fig. 7 shows a plot of $-\log C/C_0$ *versus* time. The rate constant k calculated for 6 ppm Fe^{3+} solution is 1.8×10^{-2} min^{-1}, which is three times higher than that of k calculated for 2 ppm Fe^{3+} (0.6×10^{-2} min^{-1}). The linearity in the above plot for 2 and 6 ppm Fe^{3+} ions shows two stages indicating that kinetics of photo catalytic decomposition of CR follows two stages of first order rate. The rate constant in the first stage is nominal compared to the second stage. These values are shown in Table 2. When the concentration of iron is ≥ 10 ppm, reaction deviates from first order kinetics and follows zero order. Catalytic efficiency (k_c) is a kinetic parameter that is calculated using the formula

$$k_c = \frac{k^1 - k_0}{[Fe^{3+}]^n} \qquad (9)$$

Where 'k_c' is the catalytic efficiency, 'k^1' is the rate constant of the reaction with catalyst, 'k_0' is the rate constant of the reaction without catalyst. 'n' is the order of the reaction and Fe^{3+} is the concentration of the catalyst used.

Table 2 shows the catalytic efficiency calculated for different concentration of catalyst. 2 and 6 ppm Fe^{3+} ion concentration shows higher catalytic efficiency. The value decreases for higher concentrations due to the following reasons: (1) At high concentration of Fe^{3+} ions the concentration of aqua complex Fe $[OH]^{2+}$ increases. This complex has strong absorption in the UV region (280 - 400 nm). Therefore, the complex competes with Fe^{3+} ions for the photon absorption thereby decreasing the degradation rate.

(2) Excess Fe^{2+} ion concentrations shows a scavenging effect. These ions instead of enhancing the degradation rate scavenge the hydroxyl radicals and convert them to hydroxyl anions and thereby getting oxidized to Fe^{3+} ions (Eq. 7). This is also confirmed by kinetics experiments (Fig. 7). The reaction follows zero order kinetics at higher concentration of catalyst. In the initial stages of the degradation reaction, substrate concentration and Fe^{3+} ion concentration is high. They show interdependence on one another and follow first order kinetics. At the later stages of the reaction, substrate concentration decreases but the number of Fe^{3+} ions remains constant. Therefore, degradation rate follows zero order kinetics.

The efficiency of photochemical reaction can be expressed in terms of quantum yield, which is equal to the number of molecules reacted divided by the number of photons absorbed. In the present method this effectiveness of photochemical reaction is calculated using 'Process efficiency (Φ)'. The Process efficiency is defined as the change in concentration divided by the amount of energy in terms of intensity and exposure surface area per time.

$$\Phi = \frac{C_0 - C}{t.I.S} \qquad (10)$$

C_0 is the initial concentration of the substrate and C is the concentration at time 't'. (C_0- C) denotes the residual pollutant concentration in mg L^{-1} or ppm. 'I' is the irradiation intensity. 'S' denotes the solution irradiated plane surface area in cm^2 and 't' represents the irradiation time in minutes.

When the concentration of the catalyst is increased from 2 ppm to 6 ppm, process efficiency increases. With further increase in iron concentration, process efficiency decreases as shown in the Table 2. The data obtained from rate constant (k), catalytic efficiency (k_c) and Process efficiency (Φ) suggests that the present experimental design used for the degradation of CR is most efficient at lower concentration of iron.

Table 2. Rate, Rate constant (k), Catalytic efficiency (k_c) and Process efficiency (Φ) calculated for different concentration of iron catalyst.

[Fe^{3+}] in ppm	Rate (dα/dt) x 10^{-2} ppm min^{-1}	Rate Constant (k) from log C/C_0 versus time plot in min^{-1}	Catalytic efficiency ppm^{-1} min^{-1}	Process efficiency x (10^{-12}) ppm Einstein^{-1}
2	2.3	0.6×10^{-2}	0.24	22.77
6	2.6	1.8×10^{-2}	0.28	29.20
10	0.6	0.76×10^{-2}	0.06	16.35
15	0.7	0.6×10^{-2}	0.03	13.72
20	0.9	0.4×10^{-2}	0.01	9.92
0 (k_0)		0.12×10^{-2}	-	

Photo fenton like process $Fe^{3+}/(NH_4)_2S_2O_8/UV$
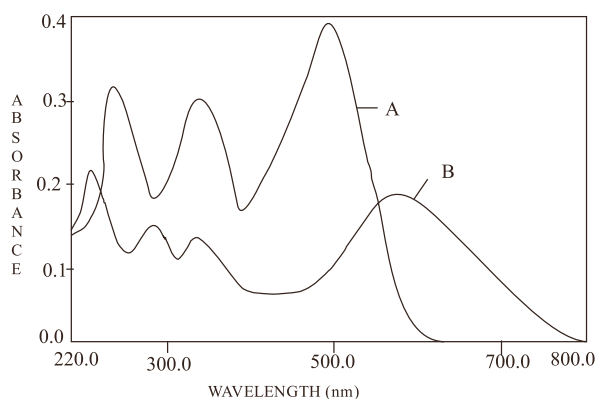for the degradation of Di azo dye congo red
using low iron concentration

Figure 8. UV-Visible spectra of CR dye A: Dye solution pH 6.6, B: Dye solution pH 3.0

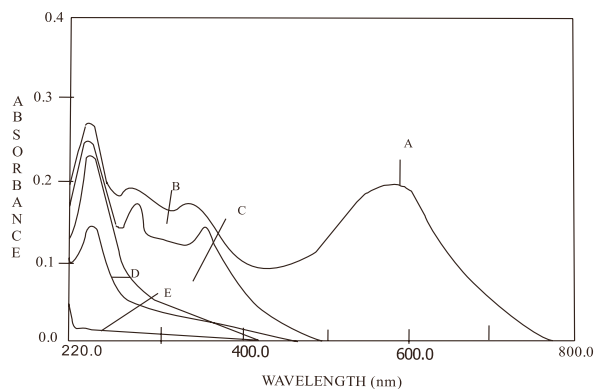**Figure 9.** UV-Visible spectra of CR dye: (A) Before irradiation, (B) At 50 minutes, (C) 2 hours, (D) 3.5 hours, (E) 5 hours; Fe^{3+} = 6 ppm, APS = 50 ppm, pH = 3 and Dye = 10 ppm
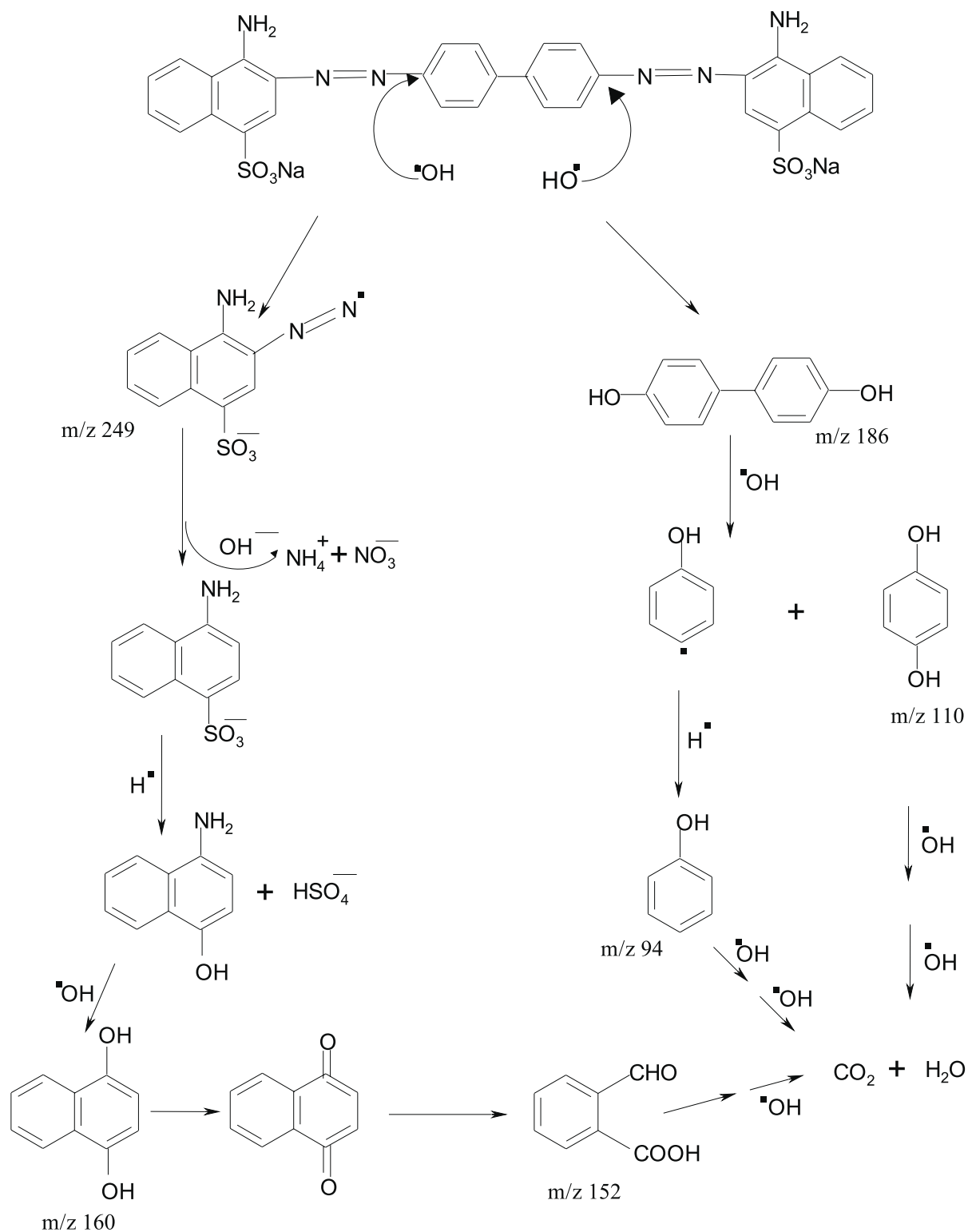
3.7 UV-visible spectroscopic analysis

The color of the dye solution changes from red to blue when the pH is lowered. The (λ_{max}) of the CR dye in the pH range 5 - 9 is 497 nm attributed to the azo form of the dye. Under acidic pH 3 due to the progressive protonation, (λ_{max}) shifts to longer wavelength (577 nm) due to the formation of azonium ion. Similar red shift is observed for the peak at 268 nm to 284 nm (Fig. 8). On irradiation along with Fe^{3+} ions and an oxidant, the band at 577 nm reduces in its intensity and completely disappears at 50 minutes resulting in the decolorization of the dye. This confirms the cleavage of azo chromophore in the dye molecule. The spectra recorded at 50 minutes shows peaks at 208, 268 and 360 nm corresponding to the aromatic intermediates formed during the process of degradation are shown in Fig. 9. The band at 208 nm and 268 nm may appear due to the formation of mono and di substituted benzene derivative, and the band at 360 nm can arise due to the naphthalene substituted derivative. At two hours of irradiation a peak at 224 nm appears, which may correspond to the mono substituted benzene derivative. This peak slowly reduces in its intensity at 3.5 hours and completely disappears at 5 hours of irradiation indicating complete mineralization of the dye. In the initial stages, the peak at 224 nm corresponds to the electronic transitions of the aromatic rings in the CR molecule. But in the later stages, the peak still persists due to the formation of phenol as an intermediate, (which is further substantiated in the GC-MS analysis).
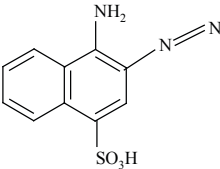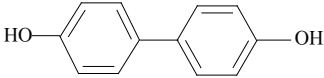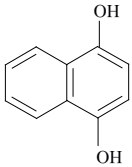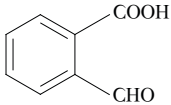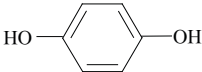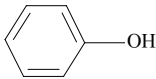
3.8 GC-MS analysis

The intermediates formed during the process of degradation are confirmed by GC-MS analysis. The GC-MS spectra show m/z peak at 651 of high intensity, which corresponds to (CR + 2H – H) species [28]. At 50 minutes, spectra showed m/z peaks of high intensity at 249, 253, 274 and 186 that appear due to cleavage of the dye molecule. The hydroxylated intermediates formed confirm the active involvement of hydroxyl radicals. The symmetrical cleavage of the molecule leads to the formation of 4,4^1-Dihydroxy biphenyl and azo radical substituted 4-Amino naphthalene sulphonic acid. The peaks at 253 and 274 are left unassigned. The GC-MS spectra recorded at 2 hours has m/z peaks of high intensity at 110 and 160 corresponding to the dihydroxy substituted benzene derivative and dihydroxy substituted naphthalene derivative. The formation of 1,4-napthalenediol may result from the loss of the azo group as NH_4^+ and NO_3^- ions and loss of SO_3^- as sulfuric acid. The resulting amino napthol yields diol by losing the -NH_2 group as NH_2OH. The other peaks at 105, 152, 165, and 178 of lower intensity are not accounted. The spectra recorded at 3.5 hours have two m/z peaks at 94 and 152, which may arise due to the formation of phenol and 2-formylbenzoic acid. The formation of the latter is probably due to the oxidation of dihydroxy substituted naphthalene to napthaquinone, followed by the loss of ethylene molecule. The spectra at 5 hours has m/z peak at 44 corresponding to CO_2, confirming the complete mineralization of the dye. Based on the UV-visible and GC-MS spectroscopic analysis, a probable reaction mechanism has been proposed (Scheme 1 & Table 3).

Scheme 1. Mechanism for degradation of CR based on UV-visible and GC-MS analysis.

Photo fenton like process Fe^{3+}/$(NH_4)_2S_2O_8$/UV
for the degradation of Di azo dye congo red
using low iron concentration

Table 3. Intermediates analyzed with their m/z peaks by GC-MS technique.

Sl.NO	m/z	Structural formula	Name of the intermediate
1	249		4-Amino, 3-azo naphthalene sulphonic acid
2	186		4,4^1, di hydroxy biphenyl
3	160		1,4 napthalene diol
4	152		2-formylbenzoic acid
5	110		Quinol (1,4 dihydroxy benzene)
6	94		Phenol

4. Conclusion

The degradation of di azo dye CR was studied by a photo assisted Fenton like process using Fe^{3+} ions and peroxy disulfate as an oxidant. The degradation rate was strongly influenced by many factors such as pH, concentration of Fe^{3+} ions / oxidant / dye. The role of hydroxyl radical in the photo Fenton like process was confirmed by performing the degradation reaction in the presence of hydroxyl radical scavenger like methyl alcohol and its effects at different concentrations were studied. It has been shown that more hydroxyl radicals can be generated using Fe(III) as a catalyst and peroxy disulfate as an oxidant. APS is chosen as an oxidant, as it provides a better acidic pH, which is most essential for Fenton's process. The rate constant (k), catalytic efficiency (k_c) and process efficiency (Φ) were calculated. These results show that the present process is quite efficient and complete mineralization of the dye can be achieved especially at lower iron concentration. At higher iron concentration, the excess Fe^{2+} ions showed a negative effect by scavenging hydroxyl radicals. Higher concentration of the dye reduces the UV light penetration into the solution thereby reducing the rate of generation of free radicals. A photo degradation pathway has been proposed based on the data obtained by the UV- visible and GC-MS spectroscopic techniques. Initially, the degradation proceeds with the formation of 4-Amino, 3-azo naphthalene sulphonic acid. The identified major intermediates are 4,4^1-dihydroxy biphenyl, cresol, phenol, naphthol and 2-formylbenzoic acid. The complete mineralization of the dye was achieved in 5 hours of UV irradiation. The present homogeneous photo Fenton process is advantageous as it introduces simple, cost effective method for the degradation of di azo dye at very low iron concentration.

Acknowledgements

References

[1] P.K. Malik, S.K. Saha, Sep. Purif. Tech. 31, 241 (2003)

[2] M. Neamtu, A. Yediler, I. Siminiiceanu, A. Kettrup, J. Photochem. Photobiol. A: Chemistry 161, 87 (2003)

[3] P. Papaolymerou, K. Ntampegliotis, A. Riga, V. Karayannis, V. Bontozoglou, J. Hazard Mater. 136, 75 (2006)

[4] S.F. Kang, C.H. Liao, M.C. Chen, Chemosphere 46, 923 (2002)

[5] S. Meric, D. Kaptan, T. Olmez, Chemosphere 54, 435 (2004)

[6] N. Daneshvar, A.R. Khataee, J. Environ. Sci. Health A 41, 315 (2006)

[7] M.P. Moya, M. Graells, L.J. Del Valle, E. Centelles, H.D. Mansilla, Catal. Today 124, 163 (2007)

[8] K. Swaminathan, S. Sandhya, A. Carmalin Sophia, K. Pachhade, Y.V. Subramanyam, Chemosphere 50, 619 (2003)

[9] J. Beltran, O. Rodriguez, J.R. Dominguez, Catal. Today 101, 389 (2005)

[10] J. Fernandez, P. Maruthmuthum J. Kiwi, J. Photochem. Photobiol. A: Chemistry 161, 185 (2004)

[11] S. Kang, C. Lio, S. Po, Chemosphere 41, 1287 (2000)

[12] M. Muruganandham, M. Swaminathan, Dyes Pigments 63, 315 (2004)

[13] M.S. Lucas, J.A. Peres, Dyes Pigments 71, 235 (2006)

[14] K. Wu, Y. Xie, J. Zhao, H. Hidaka, J. Mol. Catal. A 144, 77 (1999)

[15] M. Neamtu, A. Yediler, I. Siminiiceanu, A. Kettrup, M. Macoveanu, Dyes Pigments 60, 61 (2004)

[16] R. Liu, H.M. Chiu, C.S. Shiau, R.Y.L. Yeh, Y.T. Hung, Dyes Pigments 73, 1 (2007)

[17] C.L. Hsueh, Y.H. Huang, C.C. Wang, C.Y. Chen, Chemosphere 58, 1409 (2005)

[18] U. Pagga, D. Brown, Chemosphere 15, 479 (1986)

[19] D. Brown, B. Hamburger, Chemosphere 16, 1539 (1987)

[20] S. Chinwetkitvanich, M. Tuntoolvest, T. Panswad, Water Res. 34, 2223 (2000)

[21] G.L. Baughman, E.J. Weber, Environ. Sci. Technol. 28, 267 (1994)

[22] K. Barbusinski, J. Majewski, Polish J. Environ. Studies 12, 151 (2003)

[23] S. Ito, K. Ueno, A. Mitarai, K. Sasaki, J. Chem. Soc. Perkin Trans. 2, 255 (1993)

[24] P. Neta, V. Madhavan, H. Zemel, R.W. Fessemdem, J. Am. Chem. Soc. 99, 163 (1977)

[25] L. Gomathi Devi, S. Girish Kumar, K. Mohan Reddy, C. Munikrishnappa, J. Hazard Mater. (in press), DOI:10.1016/j.jhazmat.2008.08.017

[26] F. Banat, S.A. Asheh, A. Rawashdeh, M. Nusair, Desalination 181, 225 (2005)

[27] K. Dutta, S. Mukhopadhyay, S. Bhattacharjee, B. Chaudhuri, J. Hazard. Mater. 84, 57 (2001)

[28] S. Erdemoglu, S.K. Aksu, F. Sayilkan, B. Izgi, M. Asilturk, H. Sayilkan, F. Frimmel, S. Gucer, J. Hazard. Mater. 155, 469 (2008)